

Energy & Environmental Science

Accepted Manuscript



This is an *Accepted Manuscript*, which has been through the Royal Society of Chemistry peer review process and has been accepted for publication.

Accepted Manuscripts are published online shortly after acceptance, before technical editing, formatting and proof reading. Using this free service, authors can make their results available to the community, in citable form, before we publish the edited article. We will replace this *Accepted Manuscript* with the edited and formatted *Advance Article* as soon as it is available.

You can find more information about *Accepted Manuscripts* in the [Information for Authors](#).

Please note that technical editing may introduce minor changes to the text and/or graphics, which may alter content. The journal's standard [Terms & Conditions](#) and the [Ethical guidelines](#) still apply. In no event shall the Royal Society of Chemistry be held responsible for any errors or omissions in this *Accepted Manuscript* or any consequences arising from the use of any information it contains.

COMMUNICATION

High-Efficiency Non-Fullerene Organic Solar Cells Enabled by a Difluorobenzothiadizole-Based Donor Polymer Combined with a Properly Matched Small Molecule Acceptor

Cite this: DOI: 10.1039/x0xx00000x

Received 00th January 2012,

Accepted 00th January 2012

DOI: 10.1039/x0xx00000x

www.rsc.org/

Jingbo Zhao,^{a,§} Yunke Li,^{a,§} Haoran Lin,^{a,§} Yuhang Liu,^{a,c} Kui Jiang,^{a,b} Cheng Mu,^aTingxuan Ma,^{a,c} Joshua Yuk Lin Lai^a and He Yan^{a,b,*}

Here we report high-performance small molecule acceptor (SMA)-based organic solar cells (OSCs) enabled by the combination of a difluorobenzothiadizole donor polymer named PffBT4T-2DT and a SMA named SF-PDI₂. It is found that SF-PDI₂ matches particularly well with PffBT4T-2DT, and non-fullerene OSCs with an impressive V_{OC} of 0.98 V and a high power conversion efficiency of 6.3% are achieved. Our study shows that PffBT4T-2DT is a promising donor material for SMA-based OSCs and the selection of a matching SMA is also important to achieve the best OSC performance.

Conventional bulk-heterojunction (BHJ) organic solar cells (OSCs) are based on a polymer or small molecule material as electron donor and a fullerene derivative as electron acceptor.¹⁻⁵ Compared to inorganic solar cells, OSCs offer many attractive features including light weight, mechanical flexibility and short energy payback time.⁶ The performance of fullerene based OSCs has also been improving steadily with the power conversion efficiencies (PCEs) approaching 10% for single junction OSCs.^{4, 7-9} Despite the essential role of fullerenes in achieving best-performance OSCs, fullerene acceptors have several drawbacks including poor light absorption, high-cost production and purification.^{10, 11} For this reason, small molecule acceptor (SMA)-based OSCs have attracted much attention due to the easy tunability of electronic and optical properties of SMA materials.¹²⁻³² The performance of solution processed SMA-based OSCs has been historically low but has been improving progressively during the past few years. There have been many reports of SMA-based OSCs achieving PCEs ranging from 3.0-4.5% until a recent report of 5.9% efficiency.²⁵⁻³²

To date, much research effort in SMA-based OSCs has been focused on developing various SMA materials.^{16-22, 25-28, 31} Only limited options of polymers have been explored as the donor for SMA-based OSCs. They include P3HT and thieno[3,4-*b*]thiophene based polymers (e.g. PBDTTT-C-T³³, PTB7-Th⁷). To achieve the best performance for SMA-based OSCs, it is also highly important to select suitable donor polymers, which play a critical role in

determining the morphology and open circuit voltage (V_{OC}) of OSCs. Among the various donor polymers developed for polymer:fullerene OSCs, difluorobenzothiadizole (ffBT)-based polymers have been demonstrated to exhibit many advantages. For one, the difluorination of the benzothiadizole unit not only increases the crystallinity and hole transport ability of the polymer, it also lowers the polymer highest occupied molecular orbital (HOMO) level and thus increases the V_{OC} of OSCs.³⁴ In a recent report, an ffBT and quaterthiophene-based polymer was shown to exhibit not only high space charge limited current (SCLC) mobility in the vertical direction of the film but also high organic field-effect transistor (OFET) mobilities in the horizontal direction, indicating that the ffBT polymer can form an excellent 3D charge-transporting network.³⁵ These features make ffBT-based polymers one of the most attractive class of donor polymers for polymer:fullerene OSCs. However, ffBT polymers are not yet explored as the donor for SMA-based OSCs.

In this paper, we report high-efficiency SMA-based OSCs enabled by a previously reported ffBT-based donor polymer named here as PffBT4T-2DT. To achieve the highest PCE, it is highly important to select an SMA that matches well with the donor polymer in terms of electronic and optical properties. Two perylene diimide (PDI)-based SMAs were selected in our study to match with PffBT4T-2DT. When PffBT4T-2DT was combined with diPDI, a type of commonly used high-performance SMA^{26, 30, 32}, a reasonably high PCE of 5.4% was obtained. Interestingly, when PffBT4T-2DT was combined with SF-PDI₂, a known yet not widely used SMA (previous best performance of SF-PDI₂-based cell was ~2.4%)²², an impressively high V_{OC} of 0.98 V was obtained, which, combined with reasonably good short circuit current density (J_{sc}) and fill factor (FF), led to a PCE of 6.3%, the highest value of PCE reported for solution processed non-fullerene OSCs in the literature to date. This high performance was achieved without using any additive or interlayers, which would simplify the processing and optimizations of OSCs. The high V_{OC} of PffBT4T-2DT:SF-PDI₂-based cells can be attributed to the high-lying lowest unoccupied molecular orbital (LUMO) level of SF-PDI₂ relative to the HOMO level of PffBT4T-2DT. Importantly, the V_{OC} loss of PffBT4T-2DT:SF-PDI₂-based OSCs is only 0.67 V, which is among the lowest values of V_{OC} losses for OSCs. Our results demonstrate the advantage

of using SMAs to tune the energy level of the acceptor and thus achieve a high V_{OC} unattainable by combining the same polymer with fullerene acceptors.

The structures and energy levels of polymers and SMAs used in this study are shown in Fig. 1. Inverted structure BHJ OSCs were fabricated following the sequence of indium tin oxide (ITO)/ZnO/polymer:SMA/ V_2O_5 /Al. The J - V characteristics of the devices are shown in Fig. 2a and the performance parameters of the OSCs are summarized in Table 1. To better understand the high-efficiency PffBT4T-2DT:SF-PDI₂-based OSCs, we also investigate OSCs based on SF-PDI₂ and PTB7-Th, which belongs to the thieno[3,4-*b*]thiophene polymer family that is commonly used in SMA-based OSCs. These results show that PffBT4T-2DT:SF-PDI₂ is the best-performing material combination and that the matching between the donor polymer and SMA is important to achieve the best performance. While replacing SF-PDI₂ with diPDI reduces the OSC performance from 6.3% to 5.4%, replacing PffBT4T-2DT with PTB7-Th resulted in even more dramatic decrease in PCE to 3.0%. In the following, we will first discuss the performances of PffBT4T-2DT:SF-PDI₂ and PffBT4T-2DT:diPDI-based cells, followed by a comparative study of PffBT4T-2DT:SF-PDI₂ and PTB7-Th:SF-PDI₂ cells.

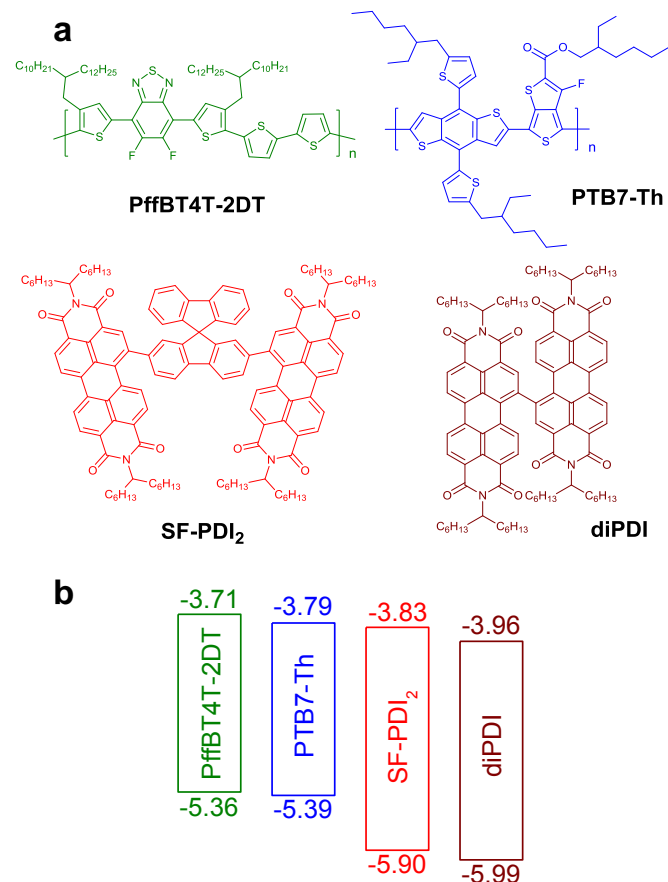


Fig. 1. (a) Chemical structures of all the materials investigated in this work. (b) Energy levels of the materials (eV). The HOMO levels were measured by cyclic voltammetry. The optical bandgaps were determined from the film absorption onsets. The LUMO levels were calculated based on HOMO levels and optical bandgaps.

There are several reasons why we chose SF-PDI₂ to match with PffBT4T-2DT. Firstly, SF-PDI₂ has a relatively high-lying LUMO

level among reported PDI-based SMAs due to the spiro-fluorene (SF) bridge. The bulky SF bridge of SF-PDI₂ also effectively reduces intermolecular aggregation and thus allows SF-PDI₂ to form films without any excessive crystallization. Furthermore, the electron transport ability of SF-PDI₂ is reasonably good among reported PDI dimers, and, as a result, the FF achieved by P3HT:SF-PDI₂-based OSCs was as high as 65%.²²

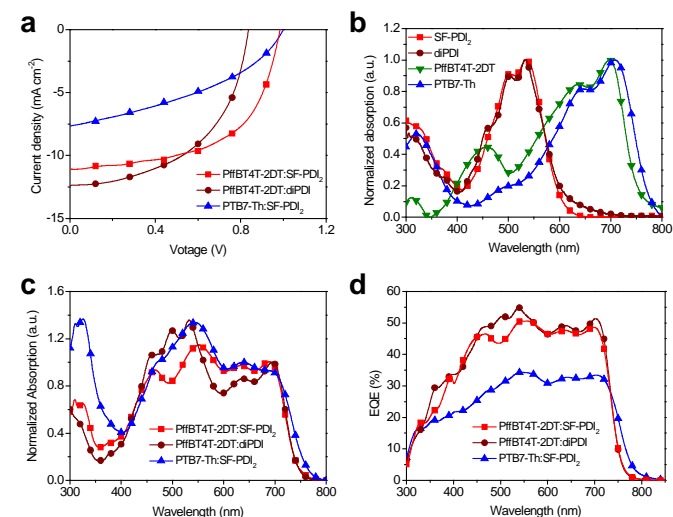


Fig. 2. (a) J - V characteristics of PffBT4T-2DT:SF-PDI₂, PffBT4T-2DT:diPDI and PTB7-Th:SF-PDI₂ devices. (b) Normalized optical absorption spectra of all the materials. (c) Normalized optical absorption spectra of PffBT4T-2DT:SF-PDI₂, PffBT4T-2DT:diPDI and PTB7-Th:SF-PDI₂ blends. All the spectra were normalized to the absorption peaks of the polymers to highlight the difference at ~450-650 nm. (d) EQE spectra of the devices.

Compared to PffBT4T-2DT:diPDI-based cells, the higher PCE of PffBT4T-2DT:SF-PDI₂-based cells can be partially explained by their higher V_{OC} , which can be attributed to the high-lying LUMO level (-3.83 eV) of SF-PDI₂ over diPDI (-3.96 eV). The difference in the LUMO values between SF-PDI₂ and diPDI (0.13 eV) correlates well with the difference in the V_{OC} of the corresponding OSCs (0.14 V). Importantly, the V_{OC} of 0.98 V achieved by PffBT4T-2DT:SF-PDI₂ is more than 200 mV higher than that of the PffBT4T-2DT:fullerene-based cells.³⁵ This shows an important advantage of SMA over fullerene-based OSCs, as the LUMO level of SMA materials can be more easily tuned, which provides a powerful tool to maximize the V_{OC} and minimize the V_{OC} loss of OSCs by finding the best matching SMA.

Table 1. Photovoltaic performances of the solar cells based on PffBT4T-2DT:SF-PDI₂, PffBT4T-2DT:diPDI and PTB7-Th:SF-PDI₂. The average values are from over 10 devices.

	V_{OC} [V]	J_{SC} [mA cm ⁻²]	FF	PCE [%]	Best PCE [%]
PffBT4T-2DT:SF-PDI ₂	0.98 ± 0.01	10.7 ± 0.4	0.57 ± 0.01	6.0 ± 0.3	6.3
PffBT4T-2DT:diPDI	0.84 ± 0.01	11.4 ± 0.9	0.53 ± 0.02	5.1 ± 0.3	5.4
PTB7-Th:SF-PDI ₂	1.00 ± 0.01	7.4 ± 0.2	0.39 ± 0.01	2.9 ± 0.1	3.0

In terms of optical properties, the absorption of PffBT4T-2DT is complementary to those of SF-PDI₂ or diPDI (Fig. 2b and 2c). While the absorption of PffBT4T-2DT covers 600-750 nm, the absorption of SF-PDI₂ or diPDI mainly covers 400-600 nm range. The external

quantum efficiency (EQE) spectra of the corresponding devices are shown in Fig. 2d. It can be seen that the EQE is in the range of 45–55% between 450 and 700 nm, meaning that both donor and acceptor materials contribute to J_{sc} . This is another attractive feature of SMA-based OSCs, as the optical properties of SMA materials can be readily tuned such that the donor and acceptor can cover different regions of the solar spectrum.

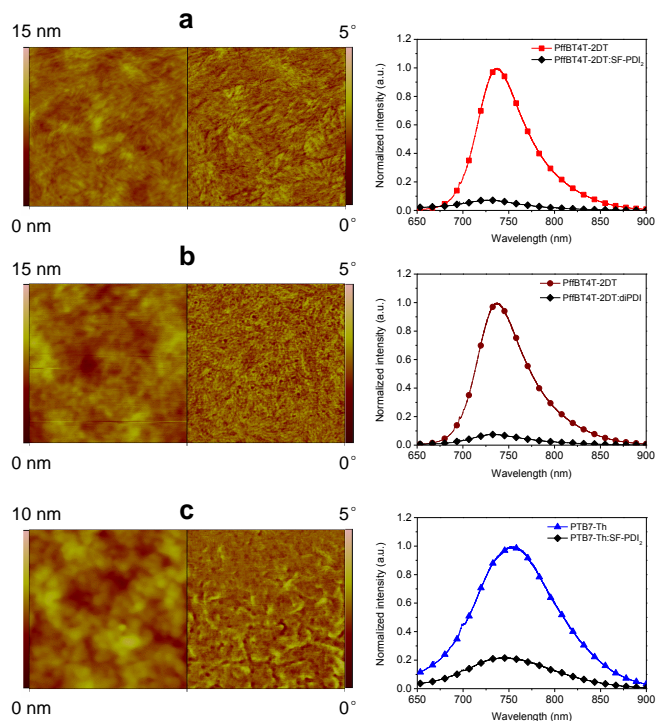


Fig. 3. AFM images ($1 \mu\text{m} \times 1 \mu\text{m}$, left) and corresponding PL quenching spectra (right) of (a) PffBT4T-2DT:SF-PDI₂ (b) PffBT4T-2DT:diPDI (c) PTB7-Th:SF-PDI₂ blends. Excitation of the films was at 633 nm. Each spectrum was corrected for the absorption of the film at the excitation wavelength.

The morphology of PffBT4T-2DT:SF-PDI₂ and PffBT4T-2DT:diPDI blend films were characterized by atomic force microscopy (AFM). The height and phase images were shown in Fig. 3. It can be seen that the surface of both PffBT4T-2DT-based blend films exhibit features of about 20–30 nm. Photoluminescence (PL) intensity of the blend films were also measured and compared with the neat polymer film (Fig. 3). The PL quenching efficiency in both PffBT4T-2DT:SF-PDI₂ and PffBT4T-2DT:diPDI blends for PffBT4T-2DT are ~93%, indicating that there is efficient exciton dissociation at the donor:acceptor interface. While AFM only probes the surface topography of the film, the high PL quenching efficiency indicates that there is good intermixing in the blend between the donor and acceptor materials.

Table 2. Hole and electron mobilities of PffBT4T-2DT:SF-PDI₂ and PffBT4T-2DT:diPDI blends.

	Hole mobility [$\text{cm}^2 \text{V}^{-1} \text{s}^{-1}$]	Electron mobility [$\text{cm}^2 \text{V}^{-1} \text{s}^{-1}$]
PffBT4T-2DT:SF-PDI ₂	2.3×10^{-3}	1.8×10^{-4}
PffBT4T-2DT:diPDI	1.2×10^{-3}	7.8×10^{-5}

A high-performing BHJ film should exhibit several features. Besides small domain size and high PL quenching efficiency, it is also important to form an efficient interpenetrating charge transporting network with reasonably good hole and electron mobilities. Hole only and electron only devices using PffBT4T-2DT:SF-PDI₂ or PffBT4T-2DT:diPDI were fabricated. Both the hole and electron mobilities are estimated using the SCLC method. The results are summarized in Table 2. It is clear that both blends exhibit higher hole mobilities than electron mobilities. The unbalanced hole and electron mobility is a common problem for SMA-based OSCs, as SMAs typically exhibit lower electron mobilities than the hole mobilities of donor polymers. For example, the electron mobility in the recently reported high-efficiency SMA-based OSC was $3.32 \times 10^{-5} \text{ cm}^2 \text{V}^{-1} \text{s}^{-1}$.³² In comparison, the electron mobility of PffBT4T-2DT:SF-PDI₂ is reasonably good. The electron mobility of PffBT4T-2DT:diPDI is significantly lower, which could contribute to the lower FF of PffBT4T-2DT:diPDI-based OSCs.

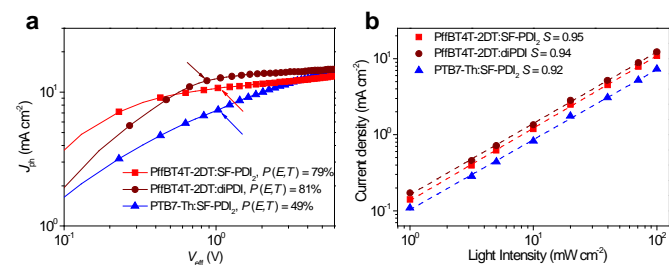


Fig. 4. (a) Photocurrent density versus effective voltage characteristics. The arrows indicate the open circuit voltage. (b) Light intensity dependence of the short circuit current of the devices. Dash lines are fits.

To understand the dramatic performance decrease of PTB7-Th:SF-PDI₂ versus PffBT4T-2DT:SF-PDI₂ cells, PL quenching experiment was conducted to investigate the exciton harvesting efficiency of the blends.^{29, 36} The PL spectra of PTB7-Th:SF-PDI₂, PffBT4T-2DT:SF-PDI₂ blends and corresponding pure polymer films are shown in Fig. 3. For the blend film of PffBT4T-2DT:SF-PDI₂, the PL quenching efficiencies of the polymer and SMA are 93% (Fig. 3a) and >96% (Fig. S1), respectively, which suggests that exciton harvesting in the PffBT4T-2DT:SF-PDI₂ blend is highly efficient. However, for PTB7-Th:SF-PDI₂, the PL emission of PTB7-Th remains relatively strong in the blend film (Fig. 3c). The PL quenching efficiency of PTB7-Th in PTB7-Th:SF-PDI₂ is calculated to be ~79% compared with 93% for PffBT4T-2DT in the PffBT4T-2DT:SF-PDI₂ blend. The lower PL quenching efficiency of PTB7-Th:SF-PDI₂ is due to, among other reasons, the relatively large domain sizes of the PTB7-Th:SF-PDI₂ blend film. AFM images of the PTB7-Th:SF-PDI₂ blend films exhibit feature sizes of about 50–60 nm, while the features on PffBT4T-2DT:SF-PDI₂ blend films are only 20–30 nm. Further studies were carried out by plotting the photocurrent density (J_{ph} , defined as $J_L - J_D$, where J_L and J_D are the current densities under illumination and in the dark, respectively) as a function of effective voltage (V_{eff} , defined as $V_0 - V$, where V_0 is the voltage at which J_{ph} is zero.) in Fig. 4a following protocols established in previous reports.^{30, 36–38} The calculated charge dissociation probabilities $P(E, T)$ for the devices of PffBT4T-2DT:SF-PDI₂ and PTB7-Th:SF-PDI₂ are 79% and 49%, respectively, which is another factor that contributes to the lower EQE of PTB7-Th:SF-PDI₂-based OSCs. As discussed in previous studies, lower charge dissociation probability is related to stronger geminate recombination at the donor:acceptor interface in BHJ blend film.^{39, 40} Lastly, light intensity dependent J_{sc} data are shown in Fig. 4b. The

relationship of between J_{SC} and light intensity can be described by the formula of $J_{SC} \propto P^S$. If all free carriers are swept out and collected at the electrodes prior to recombination, S should be equal to 1. On the other hand, an S value of < 1 indicates some extent of bimolecular recombination.^{32, 36, 37} The calculated S values for PffBT4T-2DT:SF-PDI₂ and PTB7-Th:SF-PDI₂ devices are 0.95 and 0.92, respectively. From these data, the bimolecular recombination in PffBT4T-2DT:SF-PDI₂ is quite weak, while that in PTB7-Th:SF-PDI₂ is slightly stronger. All these factors combined provide a reasonably good explanation why PTB7-Th:SF-PDI₂ does not perform as well as PffBT4T-2DT:SF-PDI₂, which again indicates the importance of matching SF-PDI₂ with a suitable donor polymer.

Furthermore, the favourable BHJ morphology and good OSC performances for PffBT4T-2DT-based cells were achieved by processing the warm solution of the PffBT4T-2DT:SMA blends without using any additives. To provide some context, the commonly reported SMA-based OSCs were fabricated by spincoating the room temperature solution of the blend, which often contains 0.4-5.0% of single or binary additives such as 1,8-diiodooctane (DIO) and 1-chloronaphthalene (CN).^{25-28, 30, 32} For polymer:fullerene OSCs, the effects of DIO have been well studied. In some cases, DIO can enhance the aggregation of the polymer as DIO is a poor solvent for the polymer.^{41, 42} Another possible effect of DIO is the reduction of the fullerene domain size because DIO is a good solvent for PC₇₁BM.^{41, 42} For SMA-based OSCs, although the use of additives is not uncommon, the detailed reasons how additives enhance device performances are not completely clear. In principle, the exact mechanism of how additive works could be material-dependent. It depends on the aggregation properties of the polymer and the relative solubility of the SMA in the additives and the processing solvent. One possible hypothesis proposed was that the DIO additive takes a long time to dry and increases the crystallinity of the SMA, which is beneficial for charge transport and OSC performance.⁴³ Recently, specially tailored binary additives including both DIO and CN were developed²⁶ and studied³⁰ to achieve excellent SMA OSC performances. Similar binary additives were also used in the best-efficiency SMA-based OSCs.³² Our current study offers a different and simpler approach (without using any additives) to obtain reasonably high-performing polymer:SMA BHJ films, which are characterized by small domain sizes and high PL quenching efficiencies. It is interesting to note that the hole mobility of PffBT4T-2DT in the SMA blend is reasonably high even without using any additives. This can be attributed to the excellent charge transport ability of the PffBT4T-2DT polymer originated from the very strong interchain aggregation of the polymer in solution.³⁵

To conclude, we demonstrate SMA-based OSCs with PCEs ranging from 5.4-6.3% enabled by an fffBT-based donor polymer (PffBT4T-2DT). The best efficiency (6.3%) was achieved by matching PffBT4T-2DT with a known yet not widely used SMA named SF-PDI₂ that exhibits a high-lying LUMO level and thus enables an impressively high V_{oc} of 0.98 V, which is the main reason why PffBT4T-2DT:SF-PDI₂ yielded higher efficiency than PffBT4T-2DT:diPDI-based cells. The two PffBT4T-2DT-based blends both exhibit relatively smooth blend morphology and highly efficient PL quenching, which are important to achieve high J_{SC} and efficiencies. Our comparative study shows that replacing PffBT4T-2DT with PTB7-Th caused a dramatic decrease in cell efficiency due to the several reasons including less favourable morphology and less efficient PL quenching of the PTB7-Th:SF-PDI₂ blend. In addition, the favourable BHJ morphology of PffBT4T-2DT-based blends was achieved by processing the warm solution of PffBT4T-2DT:SMA without using any additives, which could simplify the device

fabrication and optimization for SMA-based OSCs. Our study shows that PffBT4T-2DT is a promising donor polymer for SMA-based OSCs and that appropriate matching between the polymer and SMA is important to achieve SMA-based OSCs with high V_{oc} , J_{sc} and PCE.

Acknowledgements

The work described in this paper was partially supported by the National Basic Research Program of China (973 Program; 2013CB834701), and a grant from the Research Grants Council of the Hong Kong Special Administrative Region, China, under Theme-based Research Scheme through Project No. T23-407/13-N.

Notes and references

^a Department of Chemistry, The Hong Kong University of Science and Technology, Clear Water Bay, Hong Kong.

^b HKUST-Shenzhen Research Institute, No. 9 Yuexing 1st RD, Hi-tech Park, Nanshan, Shenzhen 518057, China.

^c Joint School of Sustainable Development, Xi'an Jiaotong University, No. 28 Xian Ning Xi Lu, Shanxi, China.

[§]These authors contributed equally.

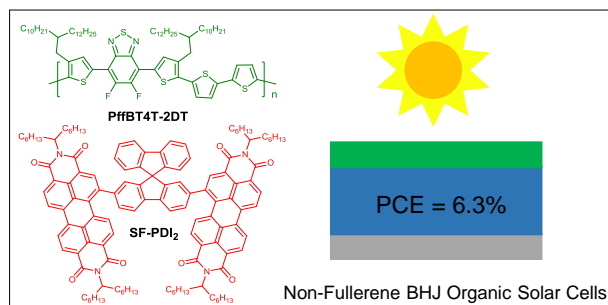
[†] Electronic Supplementary Information (ESI) available: Materials and methods, Fig. S1 to S7 and Table S1 to S2 are included. See DOI: 10.1039/c000000x/

* Corresponding author: hyan@ust.hk

1. G. Yu, J. Gao, J. C. Hummelen, F. Wudl and A. J. Heeger, *Science*, 1995, **270**, 1789-1791.
2. H. Y. Chen, J. H. Hou, S. Q. Zhang, Y. Y. Liang, G. W. Yang, Y. Yang, L. P. Yu, Y. Wu and G. Li, *Nat. Photon.*, 2009, **3**, 649-653.
3. X. G. Guo, N. J. Zhou, S. J. Lou, J. Smith, D. B. Tice, J. W. Hennek, R. P. Ortiz, J. T. L. Navarrete, S. Y. Li, J. Strzalka, L. X. Chen, R. P. H. Chang, A. Facchetti and T. J. Marks, *Nat. Photon.*, 2013, **7**, 825-833.
4. Z. C. He, C. M. Zhong, S. J. Su, M. Xu, H. B. Wu and Y. Cao, *Nat. Photon.*, 2012, **6**, 591-595.
5. J. B. You, L. T. Dou, K. Yoshimura, T. Kato, K. Ohya, T. Moriarty, K. Emery, C. C. Chen, J. Gao, G. Li and Y. Yang, *Nat. Commun.*, 2013, **4**, 1446.
6. S. B. Darling and F. You, *RSC Adv.*, 2013, **3**, 17633-17648.
7. S. H. Liao, H. J. Jhuo, Y. S. Cheng and S. A. Chen, *Adv. Mater.*, 2013, **25**, 4766-4771.
8. L. Ye, S. Zhang, W. Zhao, H. Yao and J. Hou, *Chem. Mater.*, 2014, **26**, 3603-3605.
9. C.-Z. Li, C.-Y. Chang, Y. Zang, H.-X. Ju, C.-C. Chueh, P.-W. Liang, N. Cho, D. S. Ginger and A. K. Y. Jen, *Adv. Mater.*, 2014, **26**, 6262-6267.
10. Y. He and Y. Li, *Phys. Chem. Chem. Phys.*, 2011, **13**, 1970-1983.
11. A. Anctil, C. W. Babbitt, R. P. Raffaele and B. J. Landi, *Environ. Sci. Technol.*, 2011, **45**, 2353-2359.
12. A. F. Eftaiha, J. P. Sun, I. G. Hill and G. C. Welch, *J. Mater. Chem. A*, 2014, **2**, 1201-1213.
13. Y. Lin, Y. Li and X. Zhan, *Chem. Soc. Rev.*, 2012, **41**, 4245-4272.
14. X. Zhan, A. Facchetti, S. Barlow, T. J. Marks, M. A. Ratner, M. R. Wasielewski and S. R. Marder, *Adv. Mater.*, 2011, **23**, 268-284.
15. C. Huang, S. Barlow and S. R. Marder, *J. Org. Chem.*, 2011, **76**, 2386-2407.
16. F. G. Brunetti, X. Gong, M. Tong, A. J. Heeger and F. Wudl, *Angew. Chem. Int. Ed.*, 2010, **49**, 532-536.

17. G. Ren, E. Ahmed and S. A. Jenekhe, *Adv. Energy Mater.*, 2011, **1**, 946-953.
18. J. T. Bloking, X. Han, A. T. Higgs, J. P. Kastrop, L. Pandey, J. E. Norton, C. Risko, C. E. Chen, J.-L. Brédas, M. D. McGehee and A. Sellinger, *Chem. Mater.*, 2011, **23**, 5484-5490.
19. H. Li, F. S. Kim, G. Ren, E. C. Hollenbeck, S. Subramaniyan and S. A. Jenekhe, *Angew. Chem. Int. Ed.*, 2013, **52**, 5513-5517.
20. S. Rajaram, R. Shivanna, S. K. Kandappa and K. S. Narayan, *J. Phys. Chem. Lett.*, 2012, **3**, 2405-2408.
21. Y. Zhou, L. Ding, K. Shi, Y. Z. Dai, N. Ai, J. Wang and J. Pei, *Adv. Mater.*, 2012, **24**, 957-961.
22. Q. F. Yan, Y. Zhou, Y. Q. Zheng, J. Pei and D. H. Zhao, *Chem. Sci.*, 2013, **4**, 4389-4394.
23. B. Verreet, K. Cnops, D. Cheyns, P. Heremans, A. Stesmans, G. Zango, C. G. Claessens, T. Torres and B. P. Rand, *Adv. Energy Mater.*, 2014, **4**, 1301413.
24. K. Cnops, B. P. Rand, D. Cheyns, B. Verreet, M. A. Empl and P. Heremans, *Nat. Commun.*, 2014, **5**, 3406.
25. X. Zhang, Z. Lu, L. Ye, C. Zhan, J. Hou, S. Zhang, B. Jiang, Y. Zhao, J. Huang, S. Zhang, Y. Liu, Q. Shi, Y. Liu and J. Yao, *Adv. Mater.*, 2013, **25**, 5791-5797.
26. W. Jiang, L. Ye, X. G. Li, C. Y. Xiao, F. Tan, W. C. Zhao, J. H. Hou and Z. H. Wang, *Chem. Commun.*, 2014, **50**, 1024-1026.
27. Z. H. Lu, B. Jiang, X. Zhang, A. L. Tang, L. L. Chen, C. L. Zhan and J. N. Yao, *Chem. Mater.*, 2014, **26**, 2907-2914.
28. Y. Lin, Y. Wang, J. Wang, J. Hou, Y. Li, D. Zhu and X. Zhan, *Adv. Mater.*, 2014, **26**, 5137-5142.
29. J. T. Bloking, T. Giovenzana, A. T. Higgs, A. J. Ponc, E. T. Hoke, K. Vandewal, S. Ko, Z. Bao, A. Sellinger and M. D. McGehee, *Adv. Energy Mater.*, 2014, **4**, 1301426.
30. L. Ye, W. Jiang, W. Zhao, S. Zhang, D. Qian, Z. Wang and J. Hou, *Small*, 2014, DOI: 10.1002/smll.201401082.
31. Z. Mao, W. Senevirathna, J.-Y. Liao, J. Gu, S. V. Kesava, C. Guo, E. D. Gomez and G. Sauvage, *Adv. Mater.*, 2014, **26**, 6290-6294.
32. Y. Zang, C. Z. Li, C. C. Chueh, S. T. Williams, W. Jiang, Z. H. Wang, J. S. Yu and A. K. Jen, *Adv. Mater.*, 2014, **26**, 5708-5714.
33. L. Huo, S. Zhang, X. Guo, F. Xu, Y. Li and J. Hou, *Angew. Chem. Int. Ed.*, 2011, **50**, 9697-9702.
34. A. C. Stuart, J. R. Tumbleston, H. X. Zhou, W. T. Li, S. B. Liu, H. Ade and W. You, *J. Am. Chem. Soc.*, 2013, **135**, 1806-1815.
35. Z. Chen, P. Cai, J. Chen, X. Liu, L. Zhang, L. Lan, J. Peng, Y. Ma and Y. Cao, *Adv. Mater.*, 2014, **26**, 2586-2591.
36. Z. Li, J. D. A. Lin, H. Phan, A. Sharenko, C. M. Proctor, P. Zalar, Z. Chen, A. Facchetti and T.-Q. Nguyen, *Adv. Funct. Mater.*, 2014, DOI: 10.1002/adfm.201401367.
37. L. Lu, T. Xu, W. Chen, E. S. Landry and L. Yu, *Nat. Photon.*, 2014, **8**, 716-722.
38. V. D. Mihailetschi, L. J. A. Koster, P. W. M. Blom, C. Melzer, B. de Boer, J. K. J. van Duren and R. A. J. Janssen, *Adv. Funct. Mater.*, 2005, **15**, 795-801.
39. C. M. Proctor, S. Albrecht, M. Kuik, D. Neher and T.-Q. Nguyen, *Adv. Energy Mater.*, 2014, **4**, 1400230.
40. A. J. Heeger, *Adv. Mater.*, 2014, **26**, 10-28.
41. J. K. Lee, W. L. Ma, C. J. Brabec, J. Yuen, J. S. Moon, J. Y. Kim, K. Lee, G. C. Bazan and A. J. Heeger, *J. Am. Chem. Soc.*, 2008, **130**, 3619-3623.
42. M.-S. Su, C.-Y. Kuo, M.-C. Yuan, U. S. Jeng, C.-J. Su and K.-H. Wei, *Adv. Mater.*, 2011, **23**, 3315-3319.
43. A. Sharenko, D. Gehrig, F. Laquai and T.-Q. Nguyen, *Chem. Mater.*, 2014, **26**, 4109-4118.

Table of Contents Entry



Non-fullerene organic solar cells with power conversion efficiencies of up to 6.3% are reported using properly matched donor and acceptor.

Broader Context

Sunlight is the only renewable resource capable of meeting society's long-term energy needs. Conventional crystalline Si solar cells can achieve high efficiencies but are produced using costly and energy-consuming processes. In contrast, organic solar cell can be manufactured using high-throughput roll-to-roll printing methods and are considered a truly environmentally friendly solar cell technology. However, best-efficiency organic solar cells solely rely on fullerene derivatives that are costly to synthesize and purify and that also have other drawbacks such as poor absorption properties. For this reason, non-fullerene organic solar cells based on small molecule acceptors are actively explored as the alternative to fullerene-containing organic solar cells. State-of-the-art small molecule acceptor-based organic solar cells consist of a polymer donor and a small molecule acceptor. While extensive research has been focused on developing new small molecule acceptors, limited options of polymer donors have been explored. In this work, we utilize a difluorobenzothiadiazole-based donor polymer and achieved small molecule acceptor organic solar cells with a power conversion efficiency of 6.3%, which is a new record of solution processed non-fullerene organic solar cells reported to date. Our study provides a new material combination strategy based on which high-efficiency non-fullerene organic solar cells can be achieved.